Generalized Covariance Analysis for Partially Autonomous Deep Space Missions

Jack N. Boone*
Martin Marietta Corporation, Denver, Colorado 80201

A new covariance analysis method is presented that is suitable for the evaluation of multiple impulsive controllers acting on some stochastic process x. The method accommodates batch and sequential estimators with equal ease and accounts for time-delay effects in a natural manner. The formalism is developed in terms of a generalized state vector that is formed from the system state vector x, augmented by various fixed epoch estimates, and a data vector formed from discrete time observations of the system. Recursions are developed for time transition, measurement incorporation, and impulsive control updating of the generalized covariance matrix. Means of limiting the dimensional growth of the generalized state vector via the processes of estimator epoch adjustment and measurement vector deflation are described and the application of numerically stable matrix factorization methods to the generalized covariance recursions is outlined. The method is applied to the Magellan spacecraft to demonstrate the capability of ground-based optimal estimation and control of gyro/star scanner misalignment.

I. Introduction

ONE of the attractive features of the Kalman filter is that it provides its own estimate error covariance. However, the covariance is correct only if the model structure and a priori statistics are correct. Not long after the appearance of Kalman's well-known work,[1] a number of workers independently showed (see, e.g., Ref. 2) that the true covariance recursion for correct model structure, but incorrectly assumed statistics, is generated by the "Joseph stabilized form" of Kalman's error covariance recursion using suboptimal gains derived from the Kalman gain calculation while using the incorrect statistics. Griffin and Sage[3] were first to present a comprehensive formalism for computing the true estimate error covariance for the substantially more difficult problem where the filter model of the process as well as the statistics are incorrect. They also extended their results to include true covariance recursions for smoothers as well as filters. Thornton[4] noted that the true covariance recursion may be subject to the same numerical cancellation problems that sometimes occur in standard implementations of Kalman's filter and devised stable *U-D* matrix factorization recursions for propagating the true filter error covariance.

All of these methods compute the true error covariance of a filter design directly, i.e., the true error state vector δ is modeled or, when general modeling errors are assumed, the error state vector is augmented by the process state x itself so that the δ covariance is always a diagonal block of the augmented state covariance matrix.

A shortcoming of most traditional covariance analysis methods is that the effect of impulsive control of the state by resetting to the state estimate is not represented. It is necessary to represent the effects of such control both to keep the analysis within the bounds of validity of linearization assumptions and to provide the covariance of x appropriate for some specified estimation scheme and reset schedule. A covariance analysis formalism that incorporates impulsive control representation is best formed around an augmented state generated by augmenting the state x with the estimator state $\hat{x}$ directly rather than augmenting x with the true error state vector $\delta = \hat{x} - x$. The $x/\hat{x}$ augmented state covariance propagation is generally simpler than the x/δ formulation, especially when only some subset of the x state variables or some linear combination thereof is modeled by the estimator $\hat{x}$. The true estimate error covariance of the estimate $\hat{x}$ can be obtained, if desired, by a simple congruence transformation on the $x/\hat{x}$ augmented state covariance matrix.

When applying traditional covariance analysis techniques to nonautonomous spacecraft or aerospace systems, one encounters time delay only in the form of the minor nuisance that, in some systems, control must be based on a predicted rather than a filtered state estimate due to data transmission time to a remote processing site, additional time delay due to data processing time, and, finally, transmission time back to the system for commands to perform the control action at some specified time. Actually, these time delays are present in all systems to some degree but are frequently essentially negligible. For systems operating in deep space, however, the delays can be substantial. For example, the one-way radio propagation time for Voyager II's recent encounter with Neptune was about 4 h. Furthermore, as deep space missions become more sophisticated, it is reasonable to assume that a progressively higher degree of spacecraft autonomy will be inevitable. On the other hand, for the foreseeable future, the most computationally intensive estimation and control operations will likely be ground based. Thus, the most likely scenario for the typical future spacecraft is that it will be partially autonomous. It is clear that the traditional methods of covariance analysis are hopelessly inadequate for the general case where multiple controllers are used and the estimation and control schemes are distributed and/or delayed.

The objective of the present paper is to provide a new covariance analysis framework that is suitable for the evaluation of impulsive control schemes that utilize a general mix of batch and/or sequential estimators arbitrarily distributed in space and time with respect to the controlled stochastic process x. Section II presents the general formalism in terms of a generalized state defined as the system state x augmented by various fixed epoch estimates and a data vector formed from measurements made on the system. Recursions for updating the generalized state covariance for time transition, measurement incorporation, and impulsive control are developed. Means of limiting the dimensional growth of the generalized state vector by the processes of estimator epoch adjustment and data vector deflation are also described. Section III outlines the application of numerically stable matrix factorization methods to

Received Dec. 26, 1989; revision received July 11, 1990; accepted for publication Oct. 11, 1990.

*Senior Staff Engineer, Spacecraft Analysis Department; currently Consulting Engineer, 31205 Roberts Road, Pine, CO 80470.

the generalized covariance recursions of Sec. II. Section IV provides an example application to the Magellan spacecraft, using the generalized covariance formalism to demonstrate the capability of ground-based optimal estimation and control of gyro/star scanner misalignment.

II. Generalized Covariance Analysis

We consider the problem of predicting the performance of a stochastic process x that is controlled in discrete time by corrections generated by both real-time estimators and delayed estimators. The time delays associated with the delayed estimators are assumed to consist of data transmission times to and from a remote site plus data processing and decision making times at the remote site.

The state vector of the random process is assumed to obey the linear stochastic differential equation

$$\dot{x} = Fx + w \tag{1}$$

where x and w are n_0-tuples of random variables, F is an $n_0 \times n_0$ matrix, and the superposed dot notation denotes time derivation. It is further assumed that observations of the state are available at discrete time points in the form

$$z = Hx + v \tag{2}$$

where z and v are random vectors of measurements and measurement noise, respectively, and H is a measurement matrix with dimensions determined by conformability requirements with z and x.

The first and second moments of the initial state, process noise, and measurement noise vectors are assumed to be given by

$$E[x(0)] = E[w(\tau)] = E[v(\tau)] = 0 \tag{3}$$

$$E[x(0)w^T(\tau)] = E[x(0)v^T(\tau)] = E[x(\tau)v^T(\tau)] = 0 \tag{4}$$

$$E[x(0)x^T(0)] = P_{xx}(0) \tag{5}$$

$$E[w(t)w^T(\tau)] = S(\tau)\delta(t-\tau) \tag{6}$$

$$E[v(t)v^T(\tau)] = R(\tau)\delta(t-\tau) \tag{7}$$

where superscript T denotes matrix transposition and δ denotes the Dirac distribution. Mathematical expectation in Eqs. (3-7) and elsewhere is denoted by $E[\cdot]$.

The state estimators are assumed to be unbiased linear estimators of the form

$$\hat{x}_\alpha(s_\alpha) = A^\beta_\alpha(s_\alpha)\hat{x}_\beta(\bar{s}_\beta) + B_\alpha(s_\alpha)\bar{z}, \qquad \alpha = 1,2,\ldots,n_e \tag{8}$$

where α is an estimator index, n_e the number of state estimators, s_α the local compuation time for estimator α, and the A and B matrices are dependent on the types of estimators employed. The superposed bar on the time parameter denotes a fixed epoch time for the estimator. On the other hand, the superposed bar on z denotes the chronologically ordered concatenation of all of the measurement data vectors from Eq. (2). The notation in Eq. (8) and hereafter unless otherwise stated implies summation over repeated indices when one index is up (a superscript) and the other is down (a subscript). The form of Eq. (8) is sufficiently general to accommodate all of the linear estimators of interest and obviously includes the Kalman filter and batch and recursive weighted least squares estimators. The fixed epoch terms in Eq. (8) for $\alpha \neq \beta$ are included not as an unnecessary generality but, rather to accommodate the reference adjustments required by the application of control generated by other estimator/controllers. Greek subscripts and superscripts in the following are always estimator designator indices unless otherwise stated.

The estimators are not constrained to have the same dimensionality as x or even to estimate subsets of x directly. Rather, it is assumed that

$$M_\alpha \hat{x} = L_\alpha \hat{x}_\alpha, \qquad \alpha = 1,2,\ldots,n_e \tag{9}$$

where M_α is a selector operator and L_α is some nonsingular but otherwise arbitrary linear map appropriate for the association prescribed by Eq. (9). The superposed caret on x denotes an estimate of x.

Impulsive control of the state x by the αth controller is assumed to be realized at discrete times by

$$x^+(t_c) = x^-(t_c) + C^\beta_\alpha(t_c)\hat{x}_\beta(\bar{s}_\beta) + D_\alpha(t_c)\bar{z} + c_\alpha \tag{10}$$

where c_α is a zero-mean control realization error vector uncorrelated with the initial state and the system process and measurement noises and

$$C^\beta_\alpha(t_c) = T_\alpha L_\alpha(t_c)\hat{\Phi}_\alpha(t_c,\hat{s}_\alpha)A^\beta_\alpha(\hat{s}_\alpha) \tag{11}$$

$$D_\alpha(t_c) = T_\alpha L_\alpha(t_c)\hat{\Phi}_\alpha(t_c,\hat{s}_\alpha)B^*_\alpha(\hat{s}_\alpha) \tag{12}$$

In Eq. (10), the plus and minus superscripts on x denote after and before control, respectively, at the control time t_c. In Eqs. (11) and (12), the superposed caret on the estimator time denotes the estimate time on which the control is based, the $\hat{\Phi}$ matrices are estimator transition matrices between the times indicated, and the L_α matrices are from Eq. (9). The T_α matrices are dependent on the M_α matrices from Eq. (9) and other factors designed to bring some set of linear functions of x to desired values either at the control application time t_c or some future time. In Eq. (12), the * subscripts on B_α denote the operation of appending a zero block to the unstarred version of the matrix to make it conformable with the current dimensionality of $\bar{z}$. It is further assumed that no state variable or set of state variables in x can be controlled simultaneously by more than one controller. In the frequently occurring case where impulsive control amounts to changing the contents of certain computer memory locations, the nonzero rows of T_α are identical with the rows of $-M^T_\alpha$ corresponding to the subset of x controlled by $\hat{x}_\alpha$. A more general example is provided by the case where x represents the position and velocity deviations of a spacecraft from a reference trajectory and it is desired to impulsively change the system velocity at t_c such that the spacecraft bears some desired relationship to the reference trajectory at some later time t (e.g., interception conditions). The T_α matrix would then depend on the system transition matrix between t_c and t. The c_α term in Eq. (10) for this example would then represent delta V errors due to thrust magnitude and direction errors. In summary, the estimate $\hat{x}_\alpha$ as given by Eq. (8) is propagated from the estimate time $\hat{s}_\alpha$ to the control time t_c (via the transition matrix $\hat{\Phi}_\alpha$) then mapped (via L_α) to the subset of x modeled by the estimator as prescribed by Eq. (9) and finally mapped (via the T_α matrix) to the final applied control vector. Concrete examples of the various matrices in Eqs. (11) and (12) can be found in the Magellan application in Sec. IV.

Now, in the absence of any control action, the covariance matrix of x propagates according to

$$P_{xx}(t_{k+1}) = E[x(t_{k+1})x^T(t_{k+1})]$$
$$= \Phi(t_{k+1},t_k)P_{xx}(t_k)\Phi^T(t_{k+1},t_k) + Q(t_{k+1},t_k) \tag{13}$$

where $\Phi(t_{k+1},t_k)$ is the transition matrix for the system (1) between the discrete times t_k and t_{k+1}. The process noise covariance in Eq. (13) is given by

$$Q(t_{k+1},t_k) = \int_{t_k}^{t_{k+1}} \Phi(t_{k+1},\tau)S(\tau)\Phi^T(t_{k+1},\tau)\,d\tau \tag{14}$$

where the process noise spectral density matrix S is given by Eq. (6).

The system covariance is propagated across impulsive control action from controller α by

$$P_{x+x+} = P_{x-x-} + P_{x-\hat{x}_\beta}(C_\alpha^\beta)^T + P_{x-\tilde{z}}D_\alpha^T + C_\alpha^\beta P_{\hat{x}_\beta x-} + C_\alpha^\beta P_{\hat{x}_\beta\hat{x}_\gamma}(C_\alpha^\gamma)^T + C_\alpha^\beta P_{\hat{x}_\beta\tilde{z}}D_\alpha^T + D_\alpha P_{\tilde{z}x-} + D_\alpha P_{\tilde{z}\hat{x}_\alpha}C_\alpha^T + D_\alpha P_{\tilde{z}\tilde{z}}D_\alpha^T + P_{\alpha\alpha} \tag{15}$$

where the β and γ indices appear as both superscripts (on the C matrices) and subscripts (on the P matrices) and thus are summed over the range 1 to n_e. The control noise for controller α in Eq. (15) is assumed to have covariance given by

$$P_{\alpha\alpha} = E\begin{bmatrix} c_\alpha & c_\alpha^T \end{bmatrix} \tag{16}$$

The remaining covariance and correlation matrices in Eq. (15) can be compactly summarized by augmenting the state vector to define

$$y = \begin{Bmatrix} y_0 \\ y_1 \\ y_2 \\ \cdot \\ \cdot \\ y_{n_e} \\ y_{n_e+1} \end{Bmatrix} = \begin{Bmatrix} x(t) \\ \hat{x}_1(\bar{s}_1) \\ \hat{x}_2(\bar{s}_2) \\ \cdot \\ \cdot \\ \hat{x}_{n_e}(\bar{s}_{n_e}) \\ \tilde{z} \end{Bmatrix} \tag{17}$$

and noting that

$$P_{y_A y_B} = E\begin{bmatrix} y_A & y_B^T \end{bmatrix} \qquad A,B = 0,1,\cdots,l = n_e + 1 \tag{18}$$

encapsulates all of the covariance and correlation matrices in Eq. (15).

In the interest of notational economy, it is convenient to introduce the generalized covariance matrix given by

$$P_{yy} = E\begin{bmatrix} y & y^T \end{bmatrix} \tag{19}$$

where y is given by Eq. (17). This matrix is called a generalized covariance matrix because it contains correlation matrices defined over a variety of times (off the block diagonal) in addition to covariance matrices on the block diagonal. The data vector (the last element of y) is, of course, defined over a range of times and, in fact, is of variable dimensionality. For these reasons, y given by Eq. (17) is referred to here as a generalized state having generalized covariance given by Eq. (19). The term state vector is reserved for a vector of fixed dimensionality whose components are defined at some time that is identical for all components of the vector.

Time propagation of the generalized covariance matrix between measurement update or performance evaluation (output) times is accomplished via

$$P_{yy}(t_{k+1}) = V_0 P_{yy}(t_k) V_0^T + Q_0 \tag{20}$$

where

$$V_0 = \begin{bmatrix} \Phi(t_{k+1},t_k) & & & & \\ & I & & & \\ & & I & & \\ & & & \cdot & \\ & & & & \cdot \\ & & & & & I \end{bmatrix} \tag{21}$$

$$Q_0 = \begin{bmatrix} Q(t_{k+1},t_k) & & & & \\ & 0 & & & \\ & & 0 & & \\ & & & \cdot & \\ & & & & \cdot \\ & & & & & 0 \end{bmatrix} \tag{22}$$

The matrices in Eqs. (21) and (22) are block diagonal with the dimensionalities of the identity blocks in Eq. (21) and the zero blocks in Eq. (22) determined by the dimensionality of the associated partition of y.

Similarly, propagation of the generalized covariance across impulsive control by the αth controller is expressed by

$$P_{y+y+} = V_\alpha P_{y-y-} V_\alpha^T + Q_\alpha \tag{23}$$

where

$$V_\alpha = \begin{bmatrix} I & C_\alpha^1 & \cdot & \cdot & C_\alpha^{n_e} & D_\alpha \\ & I & & & & \\ & & I & & & \\ & & & \cdot & & \\ & & & & \cdot & \\ & & & & & I \end{bmatrix} \tag{24}$$

$$Q_\alpha = \begin{bmatrix} P_{\alpha\alpha} & & & & \\ & 0 & & & \\ & & 0 & & \\ & & & \cdot & \\ & & & & \cdot \\ & & & & & 0 \end{bmatrix} \tag{25}$$

The V_α matrix is the identity matrix except for the first block row where the nontrivial block matrix elements are given by Eqs. (11) and (12). The Q_α matrix is zero except for the control noise covariance from Eq. (16) in the first block diagonal position. The zero-zero partition of Eq. (23) is, of course, simply Eq. (15).

Measurement addition implies an increase in the dimensionality of y, and propagation of the y covariance across the measurement addition is thus carried out according to

$$P_{y+y+} = V_> P_{y-y-} V_>^T + Q_> \tag{26}$$

where

$$V_> = \begin{bmatrix} I & & & & \\ & I & & & \\ & & \cdot & & \\ & & & \cdot & \\ & & & & I \\ H & 0 & \cdot & \cdot & 0 \end{bmatrix} \tag{27}$$

$$Q_> = \begin{bmatrix} 0 & & & & \\ & 0 & & & \\ & & \cdot & & \\ & & & \cdot & \\ & & & & 0 \\ & & & & & R \end{bmatrix} \tag{28}$$

The use of plus and minus superscripts in Eq. (26) denotes after and before measurement addition, respectively. The $V_>$

matrix in Eq. (27) is a block diagonal matrix augmented by a block row whose only nonzero element is given by the measurement matrix from Eq. (2). The $Q_>$ matrix in Eq. (28) is zero except for the last block diagonal element, which is given by the measurement noise matrix from Eq. (7). The dimensionalities of the identity and zero block diagonal elements in Eqs. (27) and (28) are, of course, determined by the dimensionalities of the corresponding partitions of y in Eq. (17).

Since the state estimators $\hat{x}_\alpha$ are unbiased for the assumed set of processes, measurement addition when the local computation time s_α becomes equal to the time of the measurement can be accomplished via

$$(A_\alpha^\beta)^+ = (I - G_\alpha H_\alpha)(A_\alpha^\beta)^- \tag{29}$$

$$B_\alpha^+ = \left[(I - G_\alpha H_\alpha) B_\alpha^- \mid G_\alpha\right] \tag{30}$$

where the A and B matrices are as prescribed by Eq. (8) and H_α and G_α are estimator measurement matrices and gain matrices, respectively. The plus and minus superscripts in Eqs. (29) and (30) are with respect to the measurement time with the usual conventions (plus ⇒ after, minus ⇒ before).

The estimates are propagated between discrete times $(s_\alpha)_k$ and $(s_\alpha)_{k+1}$ by means of the relations

$$A_\alpha^\beta(k+1) = \hat{\Phi}_\alpha(k+1,k) A_\alpha^\beta(k) \tag{31}$$

$$B_\alpha(k+1) = \hat{\Phi}_\alpha(k+1,k) B_\alpha(k) \tag{32}$$

where an obvious notation suppressing direct reference to s_α is used to avoid unnecessary clutter.

Finally, to consistently account for the adjustment made to x by controller β, estimator α must be corrected according to

$$(A_\alpha^\gamma)^+ = (A_\alpha^\gamma)^- + C_{\alpha\beta}^\gamma(t_c) \tag{33}$$

$$B_\alpha^+ = B_\alpha^- + D_{\alpha\beta}(t_c) \tag{34}$$

where the plus and minus superscripts denote after and before, respectively, the control update time at $s_\alpha = t_c$, and

$$C_{\alpha\beta}^\gamma(t_c) = L_\alpha^{-1}(t_c) M_\alpha C_\beta^\gamma(t_c) \tag{35}$$

$$D_{\alpha\beta}(t_c) = L_\alpha^{-1}(t_c) M_\alpha D_\beta^*(t_c) \tag{36}$$

The superscript -1 in Eqs. (35) and (36) and elsewhere denotes matrix inversion and the plus and minus superscripts in Eqs. (33) and (34) denote after and before the reset action, respectively. The L, M, C, and D matrices in these equations are as given by Eqs. (9–12). The case $\alpha = \beta$ in Eqs. (33) and (34) describes the self-adjustment process following confirmation of the application of the control based on Eq. (10) and using Eqs. (11) and (12). The adjustment modeled by Eqs. (33) and (34) can, of course, be omitted for $\alpha \neq \beta$ when the subset of x controlled by $\hat{x}_\beta$ is not modeled by $\hat{x}_\alpha$.

Clearly, the growth of the dimensionality of y with the addition of measurement data must be limited in order to preserve reasonable computer storage and computational burdens. This is accomplished by occasional adjustment of the estimator fixed epochs followed by deflation of the z partition of y to remove measurement data that has been processed via Eq. (26) and by all estimators via Eqs. (29) and (30) and satisfies the additional condition that the data to be deleted not appear in any pending control operation given by Eqs. (23) or (33) and (34). The propagation of the generalized covariance across the epoch adjustment is given by

$$P_{y^+y^+} = V_{\{\bar{\alpha}\}} P_{y^-y^-} V_{\{\bar{\alpha}\}}^T \tag{37}$$

where the plus and minus superscripts refer to after and before epoch adjustment, respectively, and the $\{\bar{\alpha}\}$ notation denotes the subset of estimators whose epochs are adjusted (not necessarily to the same time) by Eq. (37). The block matrix elements of $V_{\{\bar{\alpha}\}}$ are given by

$$(V_{\{\bar{\alpha}\}})_{AB} = \begin{cases} A_\alpha^\beta(s_\alpha)\delta_\alpha^A\delta_B^\beta + B_\alpha^*(s_\alpha)\delta_\alpha^A\delta_B^l & A \in \{\bar{\alpha}\} \\ I_{n_A}\delta_A^B & \text{otherwise} \end{cases} \tag{38}$$

where the δ are Kronecker deltas, the A and B block matrix indices range from 0 to $l = n_e + 1$ (the full range of y partitions), and the estimator indices α and β range only from 1 to n_e. The new epoch time for the αth estimator is then given by

$$\bar{s}_\alpha^+ = s_\alpha \qquad \alpha \in \{\bar{\alpha}\} \tag{39}$$

where s_α is the estimator time appearing in Eq. (38). The estimator A and B matrices referenced to the new epoch become, for $\alpha \in \{\bar{\alpha}\}$,

$$(A_\alpha^\beta)^+ = I_{n_\alpha}\delta_\alpha^\beta \tag{40}$$

$$B_\alpha^+ = 0 \tag{41}$$

In essence, Eqs. (39–41) replace the right side of Eq. (8) by the left side at the new epoch, and Eqs. (37) and (38) establish the covariance/correlation blocks of the generalized covariance matrix appropriate for the new set of epochs.

To accomplish the measurement data deflation, it is convenient to partition $\bar{z}$ as

$$\bar{z} = \begin{Bmatrix} \bar{z}_1 \\ \bar{z}_2 \end{Bmatrix} \tag{42}$$

where the time tags of all of the $\bar{z}_1$ components are less than the new epoch times of all of the estimators and no components of $\bar{z}_1$ enter pending control operations, as described earlier. Propagation of the generalized covariance across the deletion of the $\bar{z}_1$ vector is then accomplished by

$$P_{y^+y^+} = V_< P_{y^-y^-} V_<^T \tag{43}$$

where the plus and minus superscripts refer to after and before deflation, respectively, and

$$V_< = \begin{bmatrix} I & & & & & \\ & I & & & & \\ & & \cdot & & & \\ & & & \cdot & & \\ & & & & I & \\ & & & & 0 & I_{\bar{z}_2} \end{bmatrix} \tag{44}$$

The $V_<$ matrix is a block diagonal matrix augmented by a block column whose only nonzero element is $I_{\bar{z}_2}$, an identity matrix having dimensionality determined by $\bar{z}_2$. Note that the epoch adjustment and measurement deflation stages are both noise free, i.e., $Q_{\{\bar{\alpha}\}} = Q_< = 0$.

It should be clear at this point that the generality of the foregoing formalism derives primarily from the ability of the estimator form, Eq. (8), to capture all of the effects of impulsive control over a range of times without advancing the $\bar{s}$ estimator epochs. This allows one to avoid introducing and propagating a large number of correlation matrices. Note that the estimator recursions, Eqs. (29–34), are not involved directly in the generalized covariance recursions but, rather, provide block matrix elements for them via relatively simple matrix operations. Epoch adjustment (at the analysts' disposal) transfers the information distributed among the fixed epoch times and the $\bar{z}_1$ data vector to a priori estimates relative to $\bar{z}_2$.

The generalized covariance analysis presented here substantially generalizes all of the approaches to covariance analysis known to the present author. The emphasis on computing the

controlled covariance of the x process (rather than some estimate error covariance) is considered appropriate since it is this performance measure that is important for navigation, antenna pointing, etc. If one desires the true estimate error covariance of traditional interest to filter designers, one can define the true estimate error of the αth estimator δ_α by

$$\delta_\alpha = L_\alpha(t)\hat{x}_\alpha(t) - M_\alpha x(t) \tag{45}$$

where the L_α and M_α matrices are from Eq. (9). The desired covariance then follows from the generalized covariance results via

$$P_{\delta_\alpha\delta_\alpha} = N_\alpha P_{yy} N_\alpha^T \tag{46}$$

with the elements of the block row vector N_α given by

$$(N_\alpha)_A = \begin{cases} -M_\alpha & (A=0) \\ L_\alpha A_\alpha^A(t) & (1 \le A \le n_e) \\ L_\alpha B_\alpha(t) & (A = l = n_e+1) \end{cases} \tag{47}$$

However, unless $\hat{x}_\alpha$ is synchronous with x, Eq. (46) does not represent, in general, a realizable control error covariance even in the absence of control realization errors.

Clearly, the conventional double state vector formulation for $x/\hat{x}$ can be recovered as a special case by epoch adjustment and deflation at each time step to make $\hat{x}$ synchronous with x. Also, the generalized covariance formalism is a very natural setting for the evaluation of batch estimators, especially when control leaves no residual information in $\hat{x}$. Under these circumstances, there is no a priori information to consider and the y vector is a simple concatenation of x and $\bar{z}$.

When $\hat{x}_\alpha$ is a batch estimator, the H_α observation matrices typically prescribe the relation between a set of measurements and some fixed epoch state. Therefore, the gains G_α are appropriate for measurements respecting this assumed relation. However, when control of x by some other estimator $\hat{x}_\beta$ occurs during the data span of some batch estimator $\hat{x}_\alpha$, then the data required for $\hat{x}_\alpha$ is not directly observed but must be reconstructed by removing the effects of control by $\hat{x}_\beta$. This always leads again to an expression of the form of Eq. (8) for the batch estimator in terms of the $\hat{x}(\bar{s})$ vectors and the data vector actually observed, $\bar{z}$. It may also be necessary to model other linear operations on $\bar{z}$, such as those required to generate differenced data. Examples of such derived data operations are described in Sec. IV.

In the general case, Eq. (2) represents a variety of different types of data from a variety of sources, i.e., H and R are not the same, in general, for different measurements. A given estimator $\hat{x}_\alpha$ may process all of the data or only selected subsets. Under these circumstances, significant computer storage may be saved by storing only the nonzero columns of B_α and the associated pointers to $\bar{z}$. Also, the generalized covariance matrix is symmetric and storage requirements for this large matrix can be approximately halved by storing only nonredundant matrix elements.

III. Matrix Factor Formulation

The purpose of control, of course, is to transfer information from the state estimator(s) to x. For effective estimation and control schemes, the a posteriori mean square deviation of x from its expected value [zero in this case due to Eq. (3) and the remark following Eq. (10)] is reduced in general. In some cases, the reduction of scatter or uncertainty from $P_{x^-x^-}$ to $P_{x^+x^+}$ in Eq. (15) is such that leading digit cancellation in a naive implementation of Eq. (15) can produce physically nonsensical results such as negative variances. The problem is purely numerical and occurs in any computational situation where differences of nearly equal numbers result in a loss of precision. The analogous problem for the Kalman filter error covariance matrix is well known.[5]

To preserve the positive semidefinite character of P_{yy}, it is convenient to introduce a matrix factor representation of P_{yy} such that

$$P_{yy} = WDW^T \tag{48}$$

where D is a diagonal weight factor and W is a rectangular matrix conformable with D and having row dimension $\bar{n}$, given by

$$\bar{n} = \dim(y) = \sum_0^l n_i \tag{49}$$

When P_{yy} is represented in the form of Eq. (48), then, evidently, the individual matrix elements are given by

$$(P_{yy})_{ij} = < W_{(i)} \mid W_{(j)} >_D \tag{50}$$

where the (i) subscript denotes the ith row of the matrix and the $<\cdot|\cdot>_D$ notation denotes the inner product with metric D. Clearly, if P_{yy} is initially positive semidefinite and factorization (48) can be propagated in such a manner that this property is preserved then by Eq. (50), negative variances are impossible. The desired factor update formalism is simply

$$W^+ = [V_i W^- \mid \Pi_i] \tag{51}$$

$$D^+ = \begin{bmatrix} D^- & \\ & \Sigma_i \end{bmatrix} \tag{52}$$

where $i \in \{0, \alpha, >, \{\bar{\alpha}\}, <\}$ is an appropriate selector for one of Eqs. (21), (24), (38), or (44), respectively, and Σ_i and Π_i are such that

$$Q_i = \Pi_i \Sigma_i \Pi_i^T \tag{53}$$

with the nontrivial symmetric, positive semidefinite Q_i given by Eqs. (22), (25), and (28). The plus and minus subscripts have their usual meanings of a posteriori and a priori relative to the operation generically referenced by the subscript i.

The factors given by Eqs. (51) and (52) can be repacked to $\bar{n}$-dimensional square arrays at each step using a variety of numerically stable algorithms that preserve the positive semidefinite character of the factors. Normally, the matrix factors will be chosen upper or lower triangular to enhance computational efficiency. If D is constrained to be the identity matrix, the W triangular in Eq. (48) is called a Cholesky decomposition. Weighted Cholesky (U-D or L-D) factors can also be defined that are closely related to the (unweighted) Cholesky factors. Algorithms applicable to the reduction of Eqs. (51) and (52) to a Cholesky factor form are Householder[6] and Givens[7] transformations. Numerically reliable algorithms that explicitly preserve a nonidentity D factor are modified weighted Gram-Schmidt[8] and modified Givens[9] methods. Details on the application of these algorithms to the analogous filtering and error covariance problems can be found in Refs. 4 and 5.

Computer burden for a given selection of algorithms is a rather complex function of system matrix structure, the structure chosen for W in Eq. (48), the measurement frequency and batch size, the control schedule, and the frequency of epoch adjustment and deflation. In general, trade studies using flop counts to rank several different structure/algorithm combinations are well worthwhile. It is normally both convenient and computationally efficient to combine the epoch adjustment and measurement deflation phases. Gains and measurement matrices from modern implementations of Kalman's filter are available in column and row vector form, respectively, corresponding to measurement scalar processing. This structure continues to be efficient for the covariance analysis both in the generalized covariance propagation and in the estimate recursions, Eqs. (29) and (30), where the indicated matrix manipulations can be replaced by vector inner and outer products.

IV. Application to Optimal Estimation and Control of Misalignment for the Magellan Spacecraft

The primary mission of the Magellan spacecraft is to map the surface of the planet Venus via synthetic aperture radar (SAR). Altimetry and SAR data will be obtained from a nearly polar orbit beginning in August 1990 and continuing for approximately 243 days to complete the first mapping cycle.

Autonomous three-axis attitude determination and control is employed in performing the mapping turns, star scan slews, data downlink/uplink pointing, and other maneuvers required by the mission profile. The attitude determination function on board the spacecraft is carried out by rate-integrating strapdown gyros aided by V-slit star scanner measurements. Fixed gains for suboptimally updating the attitude and gyro bias drift using the star scanner residuals are ground generated and periodically uplinked to the spacecraft. Ground-based least squares estimation for the gyro scale factor and misalignment errors is employed using star scanner measurements obtained during special maneuver/scan sequences that are designed to enhance observability of the parameters of interest. Detailed descriptions of the attitude determination and gyro bias and scale factor parameter error estimation methodologies can be found in Ref. 10. The misalignment error estimation methodology is described in Ref. 11.

The state vector describing the evolution of Magellan's attitude error consists of the body frame referenced attitude error vector (small angle approximation) augmented by gyro bias drift, misalignment, and directional scale factor errors. The truth model constructed allows not only for random walk behavior for the bias drift, scale factor, and misalignment errors, but also for short-term and long-term parameter instabilities and parameter temperature sensitivity errors. The long-term parameter instabilities are modeled as random ramps, whereas the short-term instabilities are modeled as exponentially correlated (first-order Gauss-Markov) processes with suitably chosen correlation times. The temperature sensitivity errors are modeled as random biases and combined with expected temperature histories in the error propagation process. The state vector of the truth model so constructed contains a total of 57 state variables ($n_0 = 57$) and represents the realization of Eq. (1) for Magellan. A detailed description of the model can be found in Ref. 12.

During normal mapping operations, the spacecraft performs the mapping turns around Venus orbit periapsis and performs a star scan (two stars) around orbit apoapsis. The remaining portions of the orbit are spent in Earth point attitude for data downlink/uplink. The star scans are made in an alternating pattern, i.e., positive roll rate to scan on one orbit, negative roll rate to scan on the following orbit. The spacecraft attitude history is thus approximately periodic with a period double that of the orbital period.

The star scanner measurements made during the most recent two orbit period can be denoted by $\bar{b}$ such that

$$\bar{z} = \begin{Bmatrix} (\bar{z})^- \\ \bar{b} \end{Bmatrix} \tag{54}$$

where the minus subscript on $\bar{z}$ denotes measurements collected prior to the current two-orbit period. The $\bar{b}$ vector may be further decomposed as

$$\bar{b} = \begin{Bmatrix} \bar{b}_A \\ \bar{b}_B \\ \bar{b}_C \\ \bar{b}_D \end{Bmatrix} = \begin{Bmatrix} \bar{b}_1 \\ \bar{b}_2 \end{Bmatrix} \tag{55}$$

In Eq. (55), $\bar{b}_A$ and $\bar{b}_B$ are (forward scan) data vectors for star A and star B, respectively, and the C and D descriptors denote data gathered in the reverse scan for stars B and A, respectively, where the scanner slits are illuminated in reverse (with respect to the forward scan) order. The $\bar{b}_1$ and $\bar{b}_2$ partitions in the final member of Eq. (55) are simple concatenations of $\bar{b}_A, \bar{b}_B$ and $\bar{b}_C, \bar{b}_D$, respectively. The dimensionality of the star subscripted data vectors $\bar{b}_A, \bar{b}_B$, etc., is equal to the number of active star scanner slits n_s (either two or four for the Magellan star scanner).

The onboard attitude error filter is a fixed gain Kalman-type filter. The suboptimal model state vector consists simply of the body referenced attitude error (small angle) three vector. The onboard state estimate is reset to zero after the attitude update that occurs after all slits have been scanned at each star. Since the estimate prior to scan is initially zero and is reset to zero after each scan, the A matrices in Eq. (8) and the C matrices in Eq. (11) are always zero for the Magellan onboard filter. The B_a (subscript a for onboard attitude filter) matrices are initially zero at the beginning of each scan but have a $3 \times n_s$ nonzero final block partition at the end of the scan for each star due to the measurement update/propagate recursion given by Eqs. (30) and (32). The steady-state fixed gains G_a used in Eq. (30) are ground generated using the Kalman recursion with the three state variable suboptimal model and with process noise and measurement noise design parameters tuned to give acceptable performance. The $\bar{\Phi}_a$ transition matrices required are simply direction cosine matrices relating the body frames at successive times for this simple filter model.

The simulated attitude update is performed via Eqs. (23–25) with D_a given by Eq. (12). The L_a matrix in Eq. (12) is simply the 3×3 identity matrix for this filter, whereas the T_a matrix in Eq. (12) is $n_0 \times 3$ with zeros everywhere except the first 3×3 block, which is the negative identity matrix.

The onboard bias drift (three-vector) correction is performed every other orbit at the conclusion of the second star scan in the reverse scan process. The star scanner residuals are corrected for attitude updates performed during the two-orbit period to give free propagation residuals relative to some fixed epoch such as the first slit crossing time in the $\bar{b}_A$ vector in Eq. (55). The order of the reverse scan attitude update corrected data is then reversed and differenced with the attitude update corrected forward scan data to cancel initial epoch attitude error and orthogonal misalignment errors. The difference data vector is finally premultiplied by a ground-generated gain matrix to obtain bias drift corrections. The bias drift error estimator is thus a batch estimator that uses data solely from the current two-orbit batch. The realizations of the A and C matrices are, therefore, zero for the bias drift batch filter. The D matrix realization in Eq. (12) requires 3×3 identity matrices for the L_b and $\bar{\Phi}_b$ matrices (subscript b for bias drift), respectively. The T_b matrix is $n_0 \times 3$ with zeros everywhere except for the negative 3×3 identity matrix in the block partition corresponding to the random bias portion of the bias drift representation in the truth model. Finally, the B_b matrix takes the form

$$B_b = [0 \mid \Gamma_b] \tag{56}$$

where

$$\Gamma_b = G_b K \Lambda \tag{57}$$

In Eq. (57) the $3 \times 2n_s$ G_b matrix is the precomputed bias drift gain matrix and

$$K = \left[I_{2n_s} \mid -J_{2n_s} \right] \tag{58}$$

where the J matrix is the order reversal operator (antidiagonal with unit elements on the antidiagonal). The subscripts on the identity I and order reversal matrix J indicate dimensionalities of double the number of active star scanner slits n_s. The Λ matrix in Eq. (57) is block unit lower triangular with subdiagonal blocks given by

$$(\Lambda_{\Omega\Lambda})_{ij} = H_a(t_{\Omega_i}) \bar{\Phi}_a(t_{\Omega_i}, t_{\Delta_{n_s}}) B_a^{(\Delta j)} \qquad \Delta = 1,2,3$$

$$\Delta < \Omega \leq 4; \quad i,j = 1,2,\ldots,n_s \tag{59}$$

The Ω_i subscripts on time in Eq. (59) denote the ith time in partition Ω, etc., of the $\bar{b}$ vector in Eq. (55), whereas the H_a row rectors are simply the cross product of the crossing plane unit normal with the star unit vector at the slit crossing time. The measurement corresponding to the coupling prescribed by H_a is (apart from a sign that sets the error convention) simply the dot product of the slit crossing plane unit normal with the star unit vector at the slit crossing time.[13] The $\hat{\Phi}_a$ in Eq. (59) is the onboard filter transition matrix, and the (Δ_j) superscript on the B_a matrix denotes the jth column of the nonzero partition of the B_a matrix for the Δth star scan in the current two orbit period. Stated succinctly, the Λ matrix removes the effects of attitude updates and the K matrix performs the differences required for the bias filter.

The gains for the difference data batch filters (bias drift and directional scale factors) are given by

$$G_p = (KH_p)^{\#} \qquad p \in \{b, S^+, S^-\} \tag{60}$$

where the # superscript denotes matrix pseudoinversion, K is given by Eq. (58), and the generic parameter descriptor p takes on values corresponding to bias drift (b), positive rate fractional scale factor error (S^+), and negative rate fractional scale factor error (S^-). The H_p matrices are given by

$$(H_p)_{ij} = H_a(t_i)\hat{\Phi}^{(j)}_{\theta p}(t_i, t_{A_1}) \tag{61}$$

where the t_i times correspond with the chronologically ordered slit illumination times over the period spanned by successive scans, and t_{A_1} is the first slit illumination time for star A in the $\bar{b}$ vector introduced in Eq. (55). The $\hat{\Phi}_{\theta p}$ matrices are the θp (θ = attitude error) blocks of the transition matrix for some (not necessarily optimal) state vector including the random bias parameter three vector p as an error source, and the superscript (j) notation denotes the jth column of the matrix. The B_p matrices for the scale factor batch filters ($p = S^+$ or S^-) are determined in a manner precisely analogous to the B_b matrix in Eqs. (56) and (57) via the simple prescription $b \to p$ and using Eqs. (60) and (61) corresponding to the appropriate parameter.

The ground-based filter used to estimate misalignment error is a Kalman filter having the exact structure and a priori statistics of the truth model. The optimal gains G_t (subscript t for truth) are generated from a U-D implementation[5] of the Kalman recursion. The star scanner measurements are assumed to be unbiased with 15-arc-s (1σ) white measurement noise so that the H_t matrices appropriate for the truth model filter scalar measurement update in Eqs. (29) and (30) are given by

$$H_t = H = \left[H_a \mid 0_{1\times n_0-3}\right] \tag{62}$$

where H_a is the onboard filter measurement matrix (row three vector). The truth model filter matrices, M_t and L_t in Eq. (9), are obviously $n_0 \times n_0$ identity matrices, and the $\hat{\Phi}_t$ matrix is simply the truth model transition matrix Φ.

For controlling the misalignment portion of the state using the ground-based filter estimate, the T_t matrices are $n_0 \times n_0$ zero matrices except for 3×3 negative identity matrices in the diagonal block partitions corresponding to the random bias portion of the truth model representation of the m (orthogonal) and n (nonorthogonal) misalignment error three vectors introduced in Ref. 11. When only two star scanner slits are used and a special maneuver/least squares estimation is used rather than the Kalman filter estimate, then a diagonal element in the T_{mn} (subscript mn for misalignment) matrix in Eq. (12) for controlling the orthogonal component of misalignment is zeroed to reflect no control for the poorly observable[11] m_2 component of misalignment.

Since the onboard attitude error filter retains no information in $\hat{x}_a$ after reset and the gyro parameter batch filters use no a priori information, the generalized state y_M for Magellan with a ground-based state estimator $\hat{x}_t$ is simply

$$y_M = \begin{Bmatrix} x(t) \\ \hat{x}_t(\bar{s}_t) \\ \bar{z} \end{Bmatrix} \tag{63}$$

Because of the form of Eq. (63), the truth model filter has only one A matrix in Eq. (8) and only one C matrix in Eq. (11).

The simulation proceeds in three phases: initialization, cruise phase, and, finally, the Venus mapping phase. Since $\hat{x}_t(0) = 0$ and no data is available at initialization time, the only nonzero partition of Eq. (19) is the zero-zero block, which is provided by Eq. (5) using calibration residual uncertainties.

The cruise portion of the mission prior to Venus orbit insertion is highly quiescent with the spacecraft in Earth point attitude except for star scan maneuvers once per day or, possibly later in the cruise mission, once every two days. Three special calibration maneuvers for scale factor and misalignment error are simulated in the cruise mission. The scale factor maneuvers simply involve a forward scan (two stars), rotation an integral number (four assumed) of turns about each spacecraft body axis, and, finally, a reverse scan of the same two stars. The maneuvers used in conjunction with least squares misalignment error estimation are described in Ref. 11. The B matrix for the misalignment batch estimator analogous to Eq. (56) is constructed using minimum norm misalignment gains derived from singular value decomposition of the fixed epoch measurement matrix. Simulation of these special calibrations along with the usual attitude and bias drift updates over the duration of the cruise mission yields the a priori covariance/correlation matrix for the mapping mission simulation. The spacecraft data are optimally reprocessed at a delayed time in the ground-based Kalman filter using reference adjustments consistent with the spacecraft suboptimal control via Eqs. (34) and (36) and employing $D_{t\alpha}$ ($\alpha \in \{a, b, S^+, S^-, mn\}$) appropriate for the type of control applied. No control of any type from the ground-based Kalman filter is simulated during the cruise mission.

The mapping mission generalized covariance matrix for y_M is initialized using the cruise mission final value. Transition matrices are generated from an attitude profile that is consistent with the Earth point attitude, the two attitude update stars selected, and the mapping attitude trace specified by quaternion component polynomial functions of time. Two star scanner slits are assumed to be active.

Since special maneuvers are required for the least squares calibration of scale factor and misalignment errors, mapping operations must be interrupted for such calibrations. One objective of the present simulation is to show that data from uninterrupted, normal mission operations combined with optimal ground-based processing provide excellent error estimates for controlling gyro error sources. It is thus unnecessary to lose SAR data while performing special maneuvers for calibrations.

The mapping simulation assumes then that autonomous attitude and bias drift updates are performed as usual but misalignment corrections are ground generated and uplinked at a (rather arbitrary) 10-day interval. The representation of the effects of onboard control (requiring reference adjustment in the ground filter) is carried out using Eqs. (33-36) and the specific matrix realizations given in the foregoing. The prediction interval for ground-based control is taken to be about 3 h. This time is realizable, enhances performance by using all of the available star scanner data, and minimizes the dimensional growth of y_M by permitting deflation at two orbit intervals.

The simulated $1-\sigma$ histories for the three components of the orthogonal misalignment $\boldsymbol{m}$ for 243 days of mapping are shown in Figs. 1-3. The corresponding results of the nonorthogonal misalignment vector $\boldsymbol{n}$ are shown in Figs. 4-6. The

initial uncertainties at the beginning of cruise are 1 arc-min $(1-\sigma)$ for each component of the m and n vectors. The initial values in the figures include the effect of the three special maneuver/least squares estimation sequences simulated during cruise. The times are referred to the beginning of the mapping mission. The effects of control (reset) are evidenced in the figures by step reductions in the true rms values at the 10-day reset interval. Growth of the true parameter error between resets is driven by random ramp parameter aging effects and, more important, by temperature sensitivity effects, especially during periods of high-temperature gradients. The aging and temperature sensitivity parameters are estimated but not reset. It is clear from the figures that, with the exception of the m_2 component, the misalignments can be controlled to within a few arc-seconds without special maneuvers over the duration of the mapping mission. The m_2 component in Fig. 2 stays close to its a priori value throughout the mission because only two star scanner slits are assumed active. The improved m_2 performance when all four star scanner slits are used is shown in Ref. 11.

The required computations were all carried out using the standard format of Eqs. (48) and (51–53) for the generalized covariance matrix using the explicit definitions appropriate for the possible operations: time transition, measurement update, control update, epoch adjustment, and measurement deflation. The corresponding recursions for the estimators were carried out using Eqs. (29–34) and (39–41). A *U-D* factor representation of P_{yy} was chosen for the Magellan application. The updated factors, Eqs. (51) and (52), were repacked to *U-D* form at each stage using modified Givens algorithms. Computation times for propagating the covariance over the entire 243-day mapping mission were under 5 h on a Sun workstation. These computation times could have been substantially reduced by using transition matrices and process noise

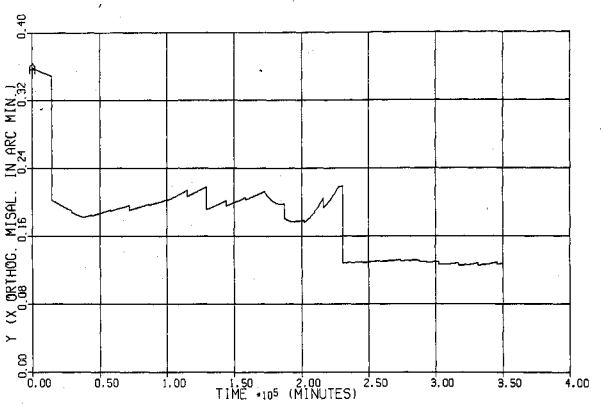

Fig. 1 Root mean squared X orthogonal misalignment m_1 history.

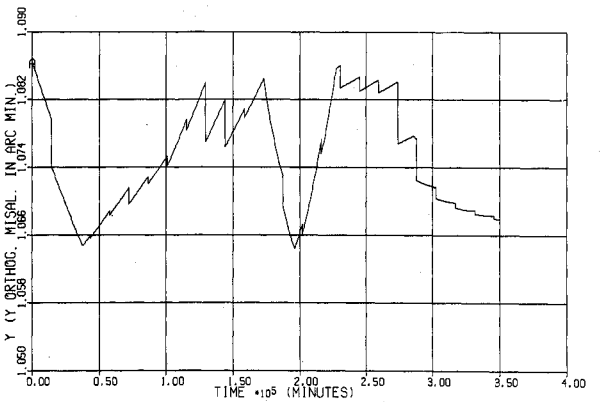

Fig. 2 Root mean squared Y orthogonal misalignment m_2 history.

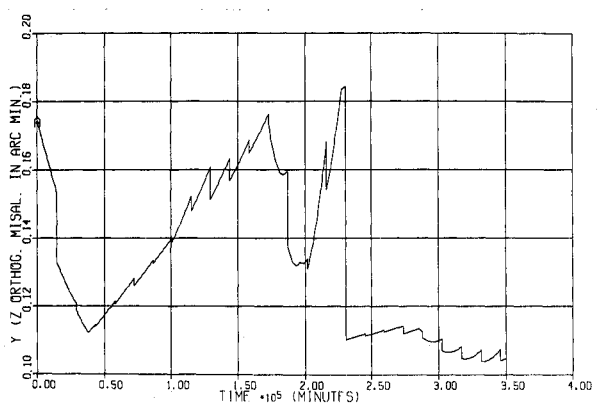

Fig. 3 Root mean squared Z orthogonal misalignment m_3 history.

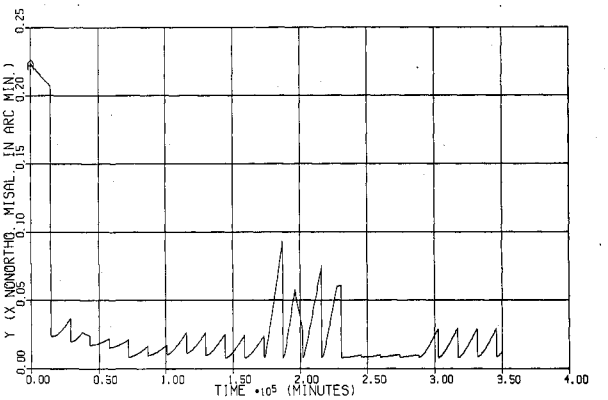

Fig. 4 Root mean squared X nonorthogonal misalignment n_1 history.

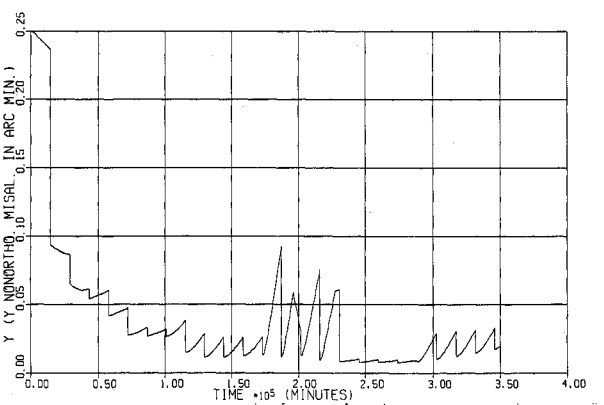

Fig. 5 Root mean squared Y nonorthogonal misalignment n_2 history.

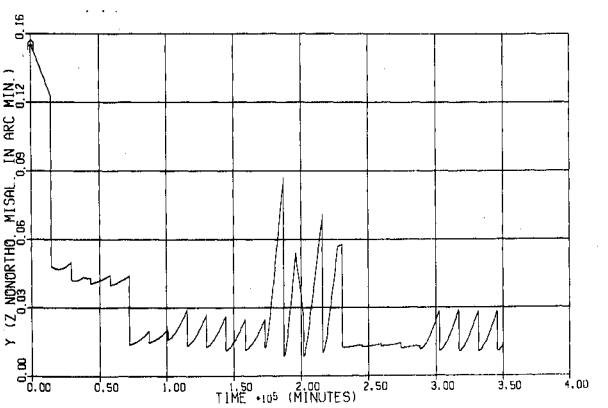

Fig. 6 Root mean squared Z nonorthogonal misalignment n_3 history.

covariance matrices from the truth model filter rather than regenerating them for the covariance recursions.

The cruise mission to date has indicated the presence of an unexpectedly high level of star scanner noise in the form of spurious slit crossing detections. The phenomenon is apparently due to energetic solar wind particles, which may act directly or in combination with a possible spacecraft charging/electrostatic surface discharge process. In any event, the measurement noise of 15 arc-s used in simulations to date has not reflected the effect of this background noise. As onboard star scanner software processing evolves to accommodate this background noise, the effective star scanner measurement noise may increase by some (to be determined) amount. In the event that this adjustment is substantial, then the noise sensitivity of some of the least squares estimation schemes for Magellan may become unacceptable and an expanded role for ground-based estimation and control would be necessary to achieve mapping and downlink attitude error requirements. Clearly, the generalized covariance simulation formalism developed in the previous sections is ideally suited for designing and evaluating such alternate schemes.

V. Summary and Conclusions

A new covariance analysis method for the design and evaluation of distributed estimation and control schemes has been developed. Novel features of the formalism are inclusion of a measurement data vector in the definition of a generalized state vector and permitting the estimator recursions to proceed asynchronously with respect to each other and the controlled process. Consequently, time delays are accommodated naturally and batch estimators are treated on an equal footing with recursive estimators.

The matrix recursions for propagating the generalized covariance can be implemented using precisely the same types of matrix factorization techniques that have proven so effective in treating numerical problems with the analogous Kalman filter problem. Numerical experience with the Magellan application indicates that matrix factor algorithms can be used reliably and efficiently with the generalized covariance recursions.

Acknowledgment

This work was performed for the Jet Propulsion Laboratory, California Institute of Technology, sponsored by NASA under Subcontract 956700.

References

[1]Kalman, R. E., "A New Approach to Linear Filtering and Prediction Problems," *Transactions of the American Society of Mechanical Engineers,* Vol. 82D, 1960, pp. 35–50.

[2]Battin, R. H., *Astronautical Guidance,* McGraw-Hill, New York, 1964.

[3]Griffin, R. E., and Sage, A. P., "Sensitivity Analysis of Discrete Filtering and Smoothing Algorithms," *AIAA Journal,* Vol. 7, No. 10, 1967, pp. 1890–1897.

[4]Thornton, C. L., "Triangular Covariance Factorizations for Kalman Filtering," Ph.D. Dissertation, UCLA School of Engineering, Dept. of Systems Science, Los Angeles, CA, 1976.

[5]Bierman, G. J., *Factorization Methods for Discrete Sequential Estimation,* Academic, New York, 1977.

[6]Householder, A. S., *The Theory of Matrices in Numerical Analysis,* Blaisdell, Waltham, MA, 1964.

[7]Givens, J. W., "Numerical Computation of the Characteristic Values of a Real Symmetric Matrix," Oak Ridge National Lab., Rept. ORNL-1574, Oak Ridge, TN, 1954.

[8]Björck, A., "Solving Least Squares Problems by Gram-Schmidt Orthogonalization," *BIT,* Vol. 7, 1967, pp. 1–21.

[9]Gentleman, W. M., "Least Squares Computation by Givens Transformations Without Square Roots," *Journal of the Institute of Mathematical Applications,* Vol. 12, 1973, pp. 329–336.

[10]Huang, H., and Reddy, N. S., "Magellan Autonomous Attitude Determination and Attitude Updates and Gyro Parameter Calibrations," AIAA Paper 86-2042, Aug. 1986.

[11]Boone, J. N., "Magellan In-Flight Gyro/Star Scanner Misalignment Calibration," *Journal of Guidance, Control, and Dynamics,* Vol. 14, No. 1, 1991, pp. 90–95.

[12]Boone, J. N., "Prediction of Attitude Error Performance for Magellan via Covariance Analysis Techniques," Martin Marietta Corp., Denver, CO, IDC 89-MGN-02-041, March 1991.

[13]Wertz, J., et al., *Attitude Determination and Control,* Reidel, Amsterdam, The Netherlands, 1980.